THE ASTRONOMICAL JOURNAL VOLUME 105, NUMBER 3 MARCH 1993

AN EXPOSURE GUIDE FOR TAKING TWILIGHT FLATFIELDS WITH LARGE FORMAT CCDS

NEIL D. TYSON[1]
Princeton University Observatory, Peyton Hall, Princeton, New Jersey 08540

ROY R. GAL[1]
Department of Astronomy, Columbia University, New York, New York 10027

Received 17 August 1992; revised 22 October 1992

ABSTRACT

Driven by the long readout times of today's large format CCDs, we present an efficient method to compute an ideal sequence of exposure times for twilight skyflats. The procedure will allow the observer to maximize the number of flats that can be obtained in the rapidly changing surface brightness of the dusk or dawn sky.

1. INTRODUCTION

Large format CCDs are now commonly used in many of the world's major observatories. Their popularity is, of course, derived from their large area, which had been the only remaining advantage of photographic over digital surveys. A major drawback, however, (aside from the disk gymnastics of managing enormous images), is the long readout time that an observer must endure at the telescope. Currently, for example, the readout time of the Tek 2048 $\times$2048 chip, available for the 0.9 m telescope at CTIO (binned 1$\times$1, with 4e^-/adu), takes nearly 4 min. While being simply a nuisance during the night, such an extended readout time steals precious minutes during dusk and dawn when twilight flatfield images are sought. As a consequence, the observer is not granted the luxury to experiment with exposure times that will properly track the rapidly changing surface brightness of the twilight sky.

The superiority of twilight flatfields over dome flatfields is well known (discussed in Buil 1992, and Mackay 1986). The entire duration of astronomical twilight is not usable for two obvious reasons, (1) when the sky is too dark then exposures will be excessively long and stars will contaminate the image, and (2) when the sky is too bright then the shortest exposures will saturate the CCD. In practice, not much more than about a third of twilight is usable to obtain flatfields. In an attempt to make the most efficient use of the available minutes, we present a simple formula that is adaptable to any telescope-filter-detector combination and to any CCD readout time. The formula properly accounts for the changing surface brightness of the twilight sky during the CCD readout and during the exposure itself. From a derived exposure sequence, the observer will be able to estimate the maximum number of flats that can be obtained during astronomical twilight.

[1]Visiting astronomer at the Cerro Tololo Inter-American Observatory, which is operated by the Associated Universities for Research in Astronomy, Inc. under contract with the National Science Foundation.

2. OBSERVATIONS

The observations were conducted at the cassegrain focus of the 0.9 m telescope at CTIO over a 6 night period from 1992 July 26–31 using the Tektronix 2048$\times$2048 No. 3 CCD chip (scale=0.445 arcsec pixel^{-1}). We were equipped with a full Harris filter set (*BVRI*) and a full Washington set (CMT_1T_2), however, twilight flatfields were obtained only for *B*, *V*, *R*, and for *C* (the bluest Washington bandpass: $\lambda_{\rm eff}$=3900 Å, FWHM=1100 Å). Each morning we took a test exposure approximately 30 min after the official onset of astronomical twilight. For efficiency, the test exposure was taken at maximum rebinning (4$\times$4 in our case), which cut readout time to under 30 s. Based on the actual counts obtained we then estimated the exposure time that would achieve our target counts of 20 000 data numbers per pixel for 1$\times$1 binning. The first flat, our "primary" exposure, was then taken using this computed time while subsequent flats were taken at varying exposures. These data appear in Table 1, where column (1) lists the local time of the exposure and column (2) lists the exposure time in seconds. Column (3) contains the average counts per pixel in data numbers over a region of the chip that was selected to be free from bad columns and traps. Column (4) contains the average flux, in counts per second per pixel. The UT date and hour angle of each set of exposures are noted for each filter.

3. DATA AND ANALYSIS

In Fig. 1 we plot our data in log *S* (with *S* in units of counts s^{-1} pixel^{-1}) vs the local time at which each twilight flat was taken. The slope of the fitted line for each filter is a measure of the time rate of change of sky surface brightness during twilight. This slope is nearly constant from bandpass to bandpass with a weighted mean: $k=0.091\pm0.006$ min^{-1}. From these data we find that the surface brightness changes by a factor of 2 about every 3 min 20 s. Although we present data from only one CCD and four filters, we expect the results to be solely a function

 0004-6256/93/031206-07$00.90

TABLE 1. Twilight flats.

Local Time (1)	exp[sec] (2)	<cts/pixel> (3)	<cts/s/pixel> (4)
B (Harris)	*26 July 1991*	*HA: +3:48*	
7:14	5	10264	2053
7:22	1	13206	13206
V (Harris)	*27 July 1992*	*HA: −2:24*	
6:59	180	23589	131
7:05	45	23827	529
7:12	10	22618	2262
7:21	2	29249	14625
C (Washington)	*29 July 1992*	*HA: 00:00 (zenith)*	
7:03	90	11879	132
7:08	45	21582	480
7:13	8	11486	1436
7:17	4	13659	3415
7:21	2	14806	7403
7:25	1	14946	14946
R (Harris)	*30 July 1992*	*HA: −4:30*	
6:45	150	18418	123
6:51	50	14622	292
6:56	20	12130	607
7:00	10	12257	1226
7:04	5	12727	2545
7:08	3	18839	6280
7:12	1	20164	20164
B (Harris)	*31 July 1992*	*HA: −3:52*	
6:56	120	25519	213
7:02	40	29235	731
7:06	10	20631	2063
7:10	3	14598	4866
7:14	1	10838	10838
7:18	1	22935	22935

of atmospheric surface brightness, and thus independent of the details of a telescope's setup.

From Fig. 1 we see that

$$\text{Log}\, S=(k/\tau)t+C, \tag{1a}$$

$$S=S_0 10^{[kt/\tau]}, \tag{1b}$$

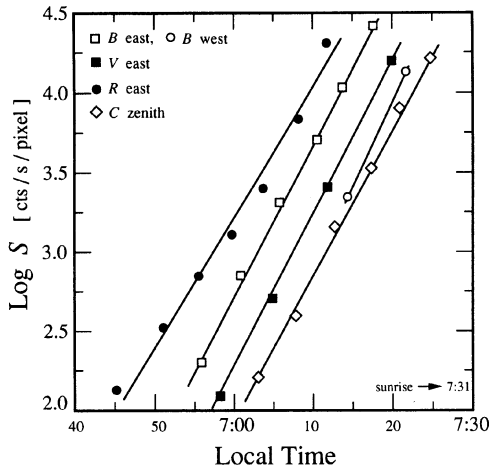

FIG. 1. Log of the twilight sky surface brightness vs local time for four broadband filters: Washington C (λ_{eff} = 3900 Å), and Harris B, V, R. All filters display a similar rate of change of surface brightness. This effect appears to be independent of direction (within 2 airmasses of the zenith) as evidenced by the similarity of slopes for data obtained while pointing east, west, and toward the zenith before sunrise.

TABLE 2. Normalized twilight durations "τ" for Northern and Southern Hemispheres.

Latitude	Spring/Autumn	Winter	Summer
0°	0.86	0.94	0.94
±15°	0.90	0.96	1.01
±30°	**1.00**	1.07	1.20
±45°	1.24	1.34	1.93
±60°	1.84	2.09	----*

* Twilight lasts all night

where S is the sky surface brightness, S_0 is the sky surface brightness at $t=0$, k is the mean slope of the plotted data, τ is the coefficient of twilight duration (discussed in the following section), t is time, and C is the scaling constant. For a uniform flatfield sequence we require that the integral of S over the exposure duration be constant, which will allow all frames to record similar mean count levels. If we define $a \equiv 10^{(k/\tau)}$, then

$$\mathscr{S}_{\text{total}}=S_0 \int_{t_i}^{t_{i+1}} a^t dt, \tag{2}$$

$$\mathbf{S}\equiv\frac{\mathscr{S}_{\text{total}}}{S_0}=\frac{a^t}{\ln(a)}\Big]_{t_i}^{t_{i+1}}. \tag{3}$$

If the primary exposure is assumed to begin at $t_0=0$, then its duration is simply t_1. This will set the value of **S**, which is in units of time, for all subsequent iterations. The parameter **S** represents what the first exposure would be if the sky surface brightness remained unchanged from the initial value S_0. Formally, $\mathscr{S}_{\text{total}}$ and S_0 each contain explicit reference to detector sensitivity, telescope size, and bandpass. Their ratio allows these dependences to cancel. Solving for t_{i+1} we may now write

$$t_{i+1}=\frac{\ln[a^{(t_i+t_{\text{ROT}})}+\mathbf{S}\ln(a)]}{\ln(a)}, \tag{4}$$

where t_{ROT} is the CCD readout time and "ln" is the natural log. The $(i+1)$ exposure duration is now simply written as

$$E_{i+1}=t_{i+1}-(t_i+t_{\text{ROT}}), \tag{5}$$

where the time delay from the CCD readout is explicitly added to the ending time of the previous exposure. Equations (4) and (5) will iteratively generate exposure times that will yield a sequence of properly exposed twilight flatfields.

4. EFFECT OF LATITUDE, SEASON, AND MOONLIGHT

The mean slope of the lines in Fig. 1 can also be interpreted as a measure of the rate at which the Sun approaches the horizon from the onset of astronomical twilight (18° below the horizon) until sunrise. Since the Sun's rising angle is not constant, we expect this rate to vary somewhat according to season and according to latitude. Table 2 gives the relative duration of twilight "τ" (adapted from the *Astronomical Almanac* 1992) for the first day of

each season at five latitudes, normalized to the 80 min of astronomical twilight on the first day of spring and of autumn at *latitude* $= \pm 30°$. These terms compensate for seasonal and latitudinal variations by appearing as divisors to the slope term in Eq. (1). Their effect is simply to scale the time axis in proportion to the total length of twilight. With the chosen twilight normalization, the appropriate slope to use in Eq. (1) becomes $k=0.094$ min^{-1}.

If the full moon were present, or if there were a large city nearby at the same azimuth as the observation, then the linearity of Eq. (1) will, of course, be valid only during that part of dawn or dusk when sunlight dominates the surface brightness of the twilight sky. It has also been brought to our attention (P. Harding, private communication) that the surface brightness relation can strongly deviate from linearity after volcanic eruptions, especially in the red and infrared.

5. EXPOSURE TABLES

We provide a sample of exposure sequences in Table 3 for CCD readout times that range from 15 s to 6 min. All sequences are computed using Eqs. (4) and (5) with $\tau=1$, and $k=0.094$ min^{-1}. The column heads identify up to 20 exposures by cardinal sequence number. The first column lists the primary exposure in seconds, from which all subsequent exposures down to 0.1 s are derived.

For the observer's convenience we have made available, via anonymous FTP to astro.princeton.edu (file: /pub/twilight.f), the FORTRAN 77 code that generated the formatted output of Table 3. Upon running the program, all the user needs to specify is either the twilight coefficient, or the duration of astronomical twilight for the latitude and date of the observing run. (Obtained, e.g., from the Sunrise/Sunset and Twilight tables in sec. A of the *Astronomical Almanac*).

Users of smaller CCDs and users of large CCDs with "quad readout" may still find the sections of Table 3 with short readout to be a useful exposure guide when planning an efficient session to obtain twilight flatfields. (For recent discussions on quad readout at NOAO see Ingerson *et al.* 1992; Walker *et al.* 1992.)

An important feature of Table 3 is that the observer need not begin a sequence at the listed primary exposure. One can begin at any exposure in the table (for a given CCD readout time) and continue the exposure sequence from there. Ultimately, however, an observer is limited by the shortest exposure allowed by the CCD controller, which is typically 1, or 0.1 s; Table 3 allows the observer to know exactly how many exposures are possible before this exposure limit is reached.

For twilight flatfields during dusk, the entries of Table 3 can, of course, be used in reverse.

6. ANALYTIC INTERPRETATION

One is prompted to ask whether the exponential rise in surface brightness of the twilight sky is consistent with what is known about the structure or content of Earth's atmosphere. Remarkably, using very basic assumptions, we can derive the slope of the surface brightness curves from the steady state "standard model" (NOAA 1976) of Earth's atmosphere. We assume that (1) the primary contribution to the surface brightness of the twilight sky is from light outside of Earth's shadow that has been scattered by the atmosphere into the line of sight. For computational simplicity, we further assume that (2) the data are taken at the zenith, which will be true for the twilight flats taken by most observers, (3) the angular dependence of Rayleigh scattering can be neglected, (4) the Sun has negligible angular extent, (5) the boundary of Earth's shadow is sharp (i.e., no penumbra), and (6) the refraction of sunlight into Earth's idealized shadow is negligible.

Following our first assumption, we presume the atmospheric *pressure* to be a direct measure of the total number of particles available to scatter sunlight into the line of sight. Consequently, we seek to compare the rate of change of atmospheric pressure at the shadow's moving boundary with our measured rate of change of twilight surface brightness. Figure 2 displays the relevant geometry, where R_0 is Earth's radius, φ is the angle (as seen from Earth's center) between the zenith observation and the point on Earth that is experiencing sunrise, and Z is the distance from Earth's surface to the boundary of Earth's shadow along the zenith as the shadow crosses the atmosphere.

Most of our data were taken while the shadow boundary dropped through the atmosphere from 400 to 100 km at the zenith. The steady state pressure profile of the standard atmosphere (NOAO 1976) at these altitudes during moderate solar activity is best fitted with a power law of the form $P(Z)=P_0Z^b$, or $\ln P=A+B\ln Z$ where A is the scaling constant and $B=-6.1$. (The atmosphere's well-known exponential profile extends only from sea level up to no more than 100 km.) The time derivative of $\ln P$ gives

$$\frac{d\ln P}{dt}=\frac{B}{Z}\frac{dZ}{dt}. \tag{6}$$

We obtain dZ/dt from the geometry of Fig. 2 where

$$\cos\varphi=R_0/(Z+R_0). \tag{7}$$

Differentiating implicitly and solving for dZ/dt gives

$$\frac{dZ}{dt}=\sin\varphi\,\frac{d\varphi}{dt}\,\frac{(Z+R_0)^2}{R_0}, \tag{8}$$

where $d\varphi/dt$ is simply Earth's rate of rotation. Substituting Eq. (8) into Eq. (6) and expanding gives

$$\frac{d\ln P}{dt}=B\sin\varphi\,\frac{d\varphi}{dt}\left(\frac{Z}{R_0}+2+\frac{R_0}{Z}\right). \tag{9}$$

For small φ and for $R_0\gg Z$ we get

$$\frac{d\ln P}{dt}=B\varphi\,\frac{d\varphi}{dt}\left(\frac{R_0}{Z}+2\right). \tag{10}$$

To compare with our data, we select $Z=250$ km as an intermediate altitude between 400 and 100 km. The corresponding φ is obtained from geometry through Eq. (7). With $R_0=6378$ km and $d\varphi/dt=-2\pi/(1440\text{ min})$ we get

TABLE 3. Exposure sequences.*

(a)

Readout time: 15 seconds Tau: 1.00

(1)	(2)	(3)	(4)	(5)	(6)	(7)	(8)	(9)	(10)	(11)	(12)	(13)	(14)	(15)	(16)	(17)	(18)	(19)	(20)
15	13.5	12.2	11.1	10.1	9.3	8.5	7.8	7.2	6.7	6.2	5.7	5.3	4.9	4.6	4.3	4.0	3.7	3.5	3.3
30	25.7	22.3	19.6	17.4	15.5	14.0	12.6	11.4	10.4	9.5	8.7	8.0	7.4	6.8	6.3	5.9	5.4	5.0	4.7
45	36.8	30.9	26.4	22.9	20.1	17.8	15.8	14.2	12.8	11.6	10.6	9.7	8.9	8.1	7.5	6.9	6.4	5.9	5.5
60	46.9	38.1	31.9	27.1	23.5	20.5	18.2	16.2	14.5	13.1	11.8	10.8	9.8	9.0	8.3	7.6	7.0	6.5	6.0
90	64.7	49.9	40.2	33.4	28.3	24.4	21.3	18.8	16.7	14.9	13.4	12.1	11.0	10.1	9.2	8.5	7.8	7.2	6.6
120	79.7	58.9	46.2	37.6	31.5	26.9	23.3	20.4	18.0	16.0	14.4	13.0	11.8	10.7	9.8	8.9	8.2	7.6	7.0
150	92.5	66.0	50.7	40.8	33.8	28.6	24.6	21.5	18.9	16.8	15.0	13.5	12.2	11.1	10.1	9.3	8.5	7.8	7.2
180	103.5	71.7	54.2	43.1	35.5	29.9	25.6	22.3	19.6	17.3	15.5	13.9	12.6	11.4	10.4	9.5	8.7	8.0	7.4
210	113.0	76.4	57.0	45.0	36.8	30.9	26.4	22.9	20.0	17.7	15.8	14.2	12.8	11.6	10.6	9.7	8.9	8.1	7.5
240	121.3	80.3	59.2	46.4	37.8	31.6	27.0	23.3	20.4	18.1	16.1	14.4	13.0	11.8	10.7	9.8	9.0	8.2	7.6
300	134.9	86.3	62.6	48.6	39.3	32.7	27.8	24.0	21.0	18.5	16.5	14.7	13.3	12.0	10.9	10.0	9.1	8.4	7.7
360	145.4	90.6	65.0	50.1	40.3	33.5	28.4	24.4	21.3	18.8	16.7	14.9	13.5	12.2	11.1	10.1	9.2	8.5	7.8

Readout time: 30 seconds Tau: 1.00

(1)	(2)	(3)	(4)	(5)	(6)	(7)	(8)	(9)	(10)	(11)	(12)	(13)	(14)	(15)	(16)	(17)	(18)	(19)	(20)
15	12.8	11.0	9.5	8.3	7.2	6.3	5.6	4.9	4.3	3.8	3.4	3.0	2.7	2.4	2.1	1.9	1.7	1.5	1.3
30	24.4	20.2	17.0	14.4	12.3	10.6	9.2	8.0	7.0	6.1	5.4	4.7	4.2	3.7	3.3	2.9	2.6	2.3	2.1
45	35.0	28.0	23.0	19.1	16.1	13.7	11.7	10.1	8.8	7.7	6.7	5.9	5.2	4.6	4.0	3.6	3.2	2.8	2.5
60	44.6	34.7	27.9	22.8	19.0	16.0	13.6	11.7	10.1	8.7	7.6	6.7	5.9	5.1	4.5	4.0	3.6	3.2	2.8
90	61.6	45.6	35.4	28.3	23.2	19.3	16.2	13.8	11.8	10.2	8.8	7.7	6.7	5.9	5.2	4.6	4.1	3.6	3.2
120	76.0	54.0	40.9	32.2	26.0	21.4	17.9	15.2	12.9	11.1	9.6	8.4	7.3	6.4	5.6	4.9	4.4	3.9	3.4
150	88.3	60.7	45.1	35.0	28.1	23.0	19.1	16.1	13.7	11.7	10.1	8.8	7.7	6.7	5.9	5.2	4.6	4.0	3.6
180	98.9	66.1	48.3	37.2	29.6	24.1	20.0	16.8	14.3	12.2	10.5	9.1	7.9	6.9	6.1	5.3	4.7	4.2	3.7
210	108.1	70.6	51.0	38.9	30.8	25.0	20.7	17.3	14.7	12.5	10.8	9.3	8.1	7.1	6.2	5.5	4.8	4.3	3.8
240	116.1	74.3	53.1	40.3	31.8	25.7	21.2	17.7	15.0	12.8	11.0	9.5	8.3	7.2	6.3	5.6	4.9	4.3	3.8
300	129.2	80.0	56.3	42.3	33.2	26.7	22.0	18.3	15.5	13.2	11.3	9.8	8.5	7.4	6.5	5.7	5.0	4.4	3.9
360	139.3	84.2	58.5	43.7	34.1	27.4	22.5	18.7	15.8	13.5	11.5	10.0	8.7	7.5	6.6	5.8	5.1	4.5	4.0

(b)

Readout time: 1 minute Tau: 1.00

(1)	(2)	(3)	(4)	(5)	(6)	(7)	(8)	(9)	(10)	(11)	(12)	(13)	(14)	(15)	(16)	(17)	(18)	(19)	(20)
15	11.5	8.9	7.0	5.5	4.4	3.5	2.8	2.2	1.8	1.4	1.1	0.9	0.7	0.6	0.5	0.4	0.3	0.2	0.2
30	22.0	16.5	12.6	9.8	7.6	6.0	4.7	3.8	3.0	2.4	1.9	1.5	1.2	1.0	0.8	0.6	0.5	0.4	0.3
45	31.6	23.1	17.3	13.2	10.2	7.9	6.2	4.9	3.9	3.1	2.5	2.0	1.6	1.3	1.0	0.8	0.7	0.5	0.4
60	40.4	28.7	21.2	15.9	12.2	9.5	7.4	5.8	4.6	3.6	2.9	2.3	1.9	1.5	1.2	1.0	0.8	0.6	0.5
90	55.9	38.0	27.3	20.2	15.2	11.7	9.1	7.1	5.6	4.4	3.5	2.8	2.2	1.8	1.4	1.1	0.9	0.7	0.6
120	69.1	45.4	31.8	23.2	17.4	13.3	10.2	8.0	6.3	4.9	3.9	3.1	2.5	2.0	1.6	1.3	1.0	0.8	0.7
150	80.5	51.2	35.3	25.5	19.0	14.4	11.1	8.6	6.7	5.3	4.2	3.3	2.7	2.1	1.7	1.4	1.1	0.9	0.7
180	90.3	56.0	38.1	27.3	20.2	15.3	11.7	9.1	7.1	5.6	4.4	3.5	2.8	2.2	1.8	1.4	1.1	0.9	0.7
210	98.8	60.0	40.4	28.7	21.2	15.9	12.2	9.5	7.4	5.8	4.6	3.6	2.9	2.3	1.9	1.5	1.2	1.0	0.8
240	106.2	63.3	42.2	29.9	21.9	16.5	12.6	9.7	7.6	6.0	4.7	3.8	3.0	2.4	1.9	1.5	1.2	1.0	0.8
300	118.4	68.5	45.0	31.6	23.1	17.3	13.2	10.2	7.9	6.2	4.9	3.9	3.1	2.5	2.0	1.6	1.3	1.0	0.8
360	127.9	72.3	47.0	32.8	23.9	17.8	13.6	10.5	8.2	6.4	5.1	4.0	3.2	2.5	2.0	1.6	1.3	1.0	0.8

Readout time: 1m 30s Tau: 1.00

(1)	(2)	(3)	(4)	(5)	(6)	(7)	(8)	(9)	(10)	(11)	(12)	(13)	(14)	(15)	(16)	(17)	(18)	(19)	(20)
15	10.4	7.3	5.1	3.7	2.6	1.9	1.3	1.0	0.7	0.5	0.4	0.3	0.2	0.1	0.1	0.1	0.1	-.-	-.-
30	19.8	13.5	9.4	6.6	4.7	3.3	2.4	1.7	1.2	0.9	0.6	0.5	0.3	0.2	0.2	0.1	0.1	0.1	-.-
45	28.5	18.9	12.9	9.0	6.3	4.5	3.2	2.3	1.6	1.2	0.9	0.6	0.4	0.3	0.2	0.2	0.1	0.1	0.1
60	36.5	23.7	15.9	11.0	7.7	5.4	3.9	2.8	2.0	1.4	1.0	0.7	0.5	0.4	0.3	0.2	0.1	0.1	0.1
90	50.7	31.6	20.8	14.1	9.8	6.9	4.9	3.5	2.5	1.8	1.3	0.9	0.7	0.5	0.3	0.2	0.2	0.1	0.1
120	62.8	37.9	24.5	16.5	11.3	7.9	5.6	4.0	2.8	2.0	1.5	1.0	0.8	0.5	0.4	0.3	0.2	0.1	0.1
150	73.2	43.0	27.4	18.3	12.5	8.7	6.1	4.3	3.1	2.2	1.6	1.1	0.8	0.6	0.4	0.3	0.2	0.2	0.1
180	82.3	47.2	29.7	19.7	13.4	9.3	6.5	4.6	3.3	2.4	1.7	1.2	0.9	0.6	0.5	0.3	0.2	0.2	0.1
210	90.1	50.7	31.6	20.8	14.1	9.8	6.9	4.9	3.5	2.5	1.8	1.3	0.9	0.7	0.5	0.3	0.2	0.2	0.1
240	97.0	53.7	33.2	21.8	14.7	10.2	7.1	5.0	3.6	2.6	1.8	1.3	1.0	0.7	0.5	0.4	0.3	0.2	0.1
300	108.4	58.3	35.6	23.2	15.6	10.8	7.5	5.3	3.8	2.7	1.9	1.4	1.0	0.7	0.5	0.4	0.3	0.2	0.1
360	117.2	61.7	37.4	24.2	16.3	11.2	7.8	5.5	3.9	2.8	2.0	1.4	1.0	0.7	0.5	0.4	0.3	0.2	0.1

TABLE 3. (continued)

(c)

Readout time: 2 minutes Tau: 1.00

(1)	(2)	(3)	(4)	(5)	(6)	(7)	(8)	(9)	(10)	(11)	(12)	(13)	(14)	(15)	(16)	(17)	(18)	(19)	(20)
15	9.3	5.9	3.8	2.4	1.6	1.0	0.6	0.4	0.3	0.2	0.1	0.1	-.-	-.-	-.-	-.-	-.-	-.-	-.-
30	17.9	11.0	6.9	4.4	2.8	1.8	1.2	0.8	0.5	0.3	0.2	0.1	0.1	0.1	-.-	-.-	-.-	-.-	-.-
45	25.7	15.5	9.6	6.1	3.9	2.5	1.6	1.0	0.7	0.4	0.3	0.2	0.1	0.1	-.-	-.-	-.-	-.-	-.-
60	33.0	19.5	11.9	7.5	4.8	3.0	2.0	1.3	0.8	0.5	0.3	0.2	0.1	0.1	0.1	-.-	-.-	-.-	-.-
90	45.9	26.2	15.7	9.8	6.2	3.9	2.5	1.6	1.0	0.7	0.4	0.3	0.2	0.1	0.1	0.1	-.-	-.-	-.-
120	57.0	31.5	18.7	11.5	7.2	4.6	2.9	1.9	1.2	0.8	0.5	0.3	0.2	0.1	0.1	0.1	-.-	-.-	-.-
150	66.5	36.0	21.1	12.9	8.0	5.1	3.3	2.1	1.3	0.9	0.6	0.4	0.2	0.2	0.1	0.1	-.-	-.-	-.-
180	74.9	39.6	23.0	14.0	8.7	5.5	3.5	2.3	1.5	0.9	0.6	0.4	0.3	0.2	0.1	0.1	-.-	-.-	-.-
210	82.1	42.7	24.5	14.8	9.2	5.8	3.7	2.4	1.5	1.0	0.6	0.4	0.3	0.2	0.1	0.1	-.-	-.-	-.-
240	88.5	45.3	25.9	15.6	9.7	6.1	3.9	2.5	1.6	1.0	0.7	0.4	0.3	0.2	0.1	0.1	-.-	-.-	-.-
300	99.0	49.4	27.9	16.7	10.3	6.5	4.1	2.7	1.7	1.1	0.7	0.5	0.3	0.2	0.1	0.1	0.1	-.-	-.-
360	107.2	52.4	29.4	17.5	10.8	6.8	4.3	2.8	1.8	1.2	0.7	0.5	0.3	0.2	0.1	0.1	0.1	-.-	-.-

Readout time: 2m 30s Tau: 1.00

(1)	(2)	(3)	(4)	(5)	(6)	(7)	(8)	(9)	(10)	(11)	(12)	(13)	(14)	(15)	(16)	(17)	(18)	(19)	(20)
15	8.4	4.8	2.7	1.6	0.9	0.5	0.3	0.2	0.1	0.1	-.-	-.-	-.-	-.-	-.-	-.-	-.-	-.-	-.-
30	16.1	9.0	5.1	2.9	1.7	1.0	0.6	0.3	0.2	0.1	0.1	-.-	-.-	-.-	-.-	-.-	-.-	-.-	-.-
45	23.2	12.7	7.1	4.1	2.3	1.4	0.8	0.5	0.3	0.2	0.1	0.1	-.-	-.-	-.-	-.-	-.-	-.-	-.-
60	29.8	16.0	8.9	5.1	2.9	1.7	1.0	0.6	0.3	0.2	0.1	0.1	-.-	-.-	-.-	-.-	-.-	-.-	-.-
90	41.5	21.6	11.8	6.7	3.8	2.2	1.3	0.7	0.4	0.2	0.1	0.1	-.-	-.-	-.-	-.-	-.-	-.-	-.-
120	51.6	26.2	14.2	7.9	4.5	2.6	1.5	0.9	0.5	0.3	0.2	0.1	0.1	-.-	-.-	-.-	-.-	-.-	-.-
150	60.4	29.9	16.1	8.9	5.1	2.9	1.7	1.0	0.6	0.3	0.2	0.1	0.1	-.-	-.-	-.-	-.-	-.-	-.-
180	68.1	33.1	17.6	9.8	5.5	3.2	1.8	1.1	0.6	0.4	0.2	0.1	0.1	-.-	-.-	-.-	-.-	-.-	-.-
210	74.7	35.8	18.9	10.4	5.9	3.4	1.9	1.1	0.7	0.4	0.2	0.1	0.1	-.-	-.-	-.-	-.-	-.-	-.-
240	80.6	38.0	20.0	11.0	6.2	3.6	2.0	1.2	0.7	0.4	0.2	0.1	0.1	-.-	-.-	-.-	-.-	-.-	-.-
300	90.3	41.6	21.6	11.9	6.7	3.8	2.2	1.3	0.7	0.4	0.2	0.1	0.1	-.-	-.-	-.-	-.-	-.-	-.-
360	97.9	44.3	22.9	12.5	7.0	4.0	2.3	1.3	0.8	0.5	0.3	0.2	0.1	0.1	-.-	-.-	-.-	-.-	-.-

(d)

Readout time: 3 minutes Tau: 1.00

(1)	(2)	(3)	(4)	(5)	(6)	(7)	(8)	(9)	(10)	(11)	(12)	(13)	(14)	(15)	(16)	(17)	(18)	(19)	(20)
15	7.5	3.9	2.0	1.0	0.5	0.3	0.1	0.1	-.-	-.-	-.-	-.-	-.-	-.-	-.-	-.-	-.-	-.-	-.-
30	14.5	7.3	3.7	1.9	1.0	0.5	0.3	0.1	0.1	-.-	-.-	-.-	-.-	-.-	-.-	-.-	-.-	-.-	-.-
45	20.9	10.3	5.3	2.7	1.4	0.7	0.4	0.2	0.1	0.1	-.-	-.-	-.-	-.-	-.-	-.-	-.-	-.-	-.-
60	26.9	13.1	6.6	3.4	1.8	0.9	0.5	0.2	0.1	0.1	-.-	-.-	-.-	-.-	-.-	-.-	-.-	-.-	-.-
90	37.5	17.8	8.9	4.5	2.3	1.2	0.6	0.3	0.2	0.1	-.-	-.-	-.-	-.-	-.-	-.-	-.-	-.-	-.-
120	46.8	21.6	10.7	5.4	2.8	1.4	0.8	0.4	0.2	0.1	0.1	-.-	-.-	-.-	-.-	-.-	-.-	-.-	-.-
150	54.8	24.8	12.2	6.1	3.2	1.6	0.9	0.4	0.2	0.1	0.1	-.-	-.-	-.-	-.-	-.-	-.-	-.-	-.-
180	61.8	27.5	13.4	6.7	3.5	1.8	0.9	0.5	0.3	0.1	0.1	-.-	-.-	-.-	-.-	-.-	-.-	-.-	-.-
210	68.0	29.8	14.4	7.2	3.7	1.9	1.0	0.5	0.3	0.1	0.1	-.-	-.-	-.-	-.-	-.-	-.-	-.-	-.-
240	73.4	31.8	15.3	7.7	3.9	2.0	1.1	0.5	0.3	0.1	0.1	-.-	-.-	-.-	-.-	-.-	-.-	-.-	-.-
300	82.3	34.9	16.7	8.3	4.3	2.2	1.1	0.6	0.3	0.2	0.1	-.-	-.-	-.-	-.-	-.-	-.-	-.-	-.-
360.0	89.3	37.3	17.7	8.8	4.5	2.3	1.2	0.6	0.3	0.2	0.1	-.-	-.-	-.-	-.-	-.-	-.-	-.-	-.-

Readout time: 3m 30s Tau: 1.00

(1)	(2)	(3)	(4)	(5)	(6)	(7)	(8)	(9)	(10)	(11)	(12)	(13)	(14)	(15)	(16)	(17)	(18)	(19)	(20)
15	6.8	3.1	1.5	0.7	0.3	0.1	0.1	-.-	-.-	-.-	-.-	-.-	-.-	-.-	-.-	-.-	-.-	-.-	-.-
30	13.0	5.9	2.7	1.3	0.6	0.3	0.1	0.1	-.-	-.-	-.-	-.-	-.-	-.-	-.-	-.-	-.-	-.-	-.-
45	18.8	8.4	3.9	1.8	0.8	0.4	0.2	0.1	-.-	-.-	-.-	-.-	-.-	-.-	-.-	-.-	-.-	-.-	-.-
60	24.2	10.7	4.9	2.3	1.1	0.5	0.2	0.1	0.1	-.-	-.-	-.-	-.-	-.-	-.-	-.-	-.-	-.-	-.-
90	33.9	14.6	6.6	3.0	1.4	0.7	0.3	0.1	0.1	-.-	-.-	-.-	-.-	-.-	-.-	-.-	-.-	-.-	-.-
120	42.3	17.8	8.0	3.7	1.7	0.8	0.4	0.2	0.1	-.-	-.-	-.-	-.-	-.-	-.-	-.-	-.-	-.-	-.-
150	49.6	20.5	9.1	4.2	1.9	0.9	0.4	0.2	0.1	-.-	-.-	-.-	-.-	-.-	-.-	-.-	-.-	-.-	-.-
180	56.1	22.8	10.1	4.6	2.1	1.0	0.5	0.2	0.1	-.-	-.-	-.-	-.-	-.-	-.-	-.-	-.-	-.-	-.-
210	61.7	24.8	10.9	5.0	2.3	1.1	0.5	0.2	0.1	0.1	-.-	-.-	-.-	-.-	-.-	-.-	-.-	-.-	-.-
240	66.7	26.5	11.6	5.3	2.4	1.1	0.5	0.2	0.1	0.1	-.-	-.-	-.-	-.-	-.-	-.-	-.-	-.-	-.-
300	74.9	29.2	12.7	5.8	2.7	1.2	0.6	0.3	0.1	0.1	-.-	-.-	-.-	-.-	-.-	-.-	-.-	-.-	-.-
360	81.4	31.3	13.5	6.1	2.8	1.3	0.6	0.3	0.1	0.1	-.-	-.-	-.-	-.-	-.-	-.-	-.-	-.-	-.-

TABLE 3. (continued)

(e)

Readout time: 4 minutes Tau: 1.00

(1)	(2)	(3)	(4)	(5)	(6)	(7)	(8)	(9)	(10)	(11)	(12)	(13)	(14)	(15)	(16)	(17)	(18)	(19)	(20)
15	6.1	2.5	1.1	0.4	0.2	0.1	-.-	-.-	-.-	-.-	-.-	-.-	-.-	-.-	-.-	-.-	-.-	-.-	-.-
30	11.7	4.8	2.0	0.8	0.4	0.1	0.1	-.-	-.-	-.-	-.-	-.-	-.-	-.-	-.-	-.-	-.-	-.-	-.-
45	17.0	6.8	2.8	1.2	0.5	0.2	0.1	-.-	-.-	-.-	-.-	-.-	-.-	-.-	-.-	-.-	-.-	-.-	-.-
60	21.8	8.7	3.6	1.5	0.6	0.3	0.1	-.-	-.-	-.-	-.-	-.-	-.-	-.-	-.-	-.-	-.-	-.-	-.-
90	30.6	11.9	4.9	2.0	0.8	0.4	0.2	0.1	-.-	-.-	-.-	-.-	-.-	-.-	-.-	-.-	-.-	-.-	-.-
120	38.3	14.7	5.9	2.5	1.0	0.4	0.2	0.1	-.-	-.-	-.-	-.-	-.-	-.-	-.-	-.-	-.-	-.-	-.-
150	44.9	16.9	6.8	2.8	1.2	0.5	0.2	0.1	-.-	-.-	-.-	-.-	-.-	-.-	-.-	-.-	-.-	-.-	-.-
180	50.8	18.9	7.6	3.1	1.3	0.5	0.2	0.1	-.-	-.-	-.-	-.-	-.-	-.-	-.-	-.-	-.-	-.-	-.-
210	56.0	20.6	8.2	3.4	1.4	0.6	0.2	0.1	-.-	-.-	-.-	-.-	-.-	-.-	-.-	-.-	-.-	-.-	-.-
240	60.5	22.0	8.8	3.6	1.5	0.6	0.3	0.1	-.-	-.-	-.-	-.-	-.-	-.-	-.-	-.-	-.-	-.-	-.-
300	68.1	24.3	9.6	4.0	1.7	0.7	0.3	0.1	0.1	-.-	-.-	-.-	-.-	-.-	-.-	-.-	-.-	-.-	-.-
360	74.1	26.1	10.3	4.2	1.8	0.7	0.3	0.1	0.1	-.-	-.-	-.-	-.-	-.-	-.-	-.-	-.-	-.-	-.-

Readout time: 4m 30s Tau: 1.00

(1)	(2)	(3)	(4)	(5)	(6)	(7)	(8)	(9)
15	5.5	2.0	0.8	0.3	0.1	-.-	-.-	-.-
30	10.5	3.9	1.5	0.5	0.2	0.1	-.-	-.-
45	15.3	5.6	2.1	0.8	0.3	0.1	-.-	-.-
60	19.7	7.1	2.6	1.0	0.4	0.1	0.1	-.-
90	27.6	9.8	3.6	1.3	0.5	0.2	0.1	-.-
120	34.6	12.0	4.4	1.6	0.6	0.2	0.1	-.-
150	40.7	13.9	5.1	1.9	0.7	0.3	0.1	-.-
180	46.0	15.6	5.7	2.1	0.8	0.3	0.1	-.-
210	50.7	17.0	6.2	2.3	0.9	0.3	0.1	-.-
240	54.9	18.2	6.6	2.4	0.9	0.3	0.1	-.-
300	61.9	20.2	7.3	2.7	1.0	0.4	0.1	0.1
360	67.3	21.7	7.8	2.9	1.1	0.4	0.2	0.1

Readout time: 5 minutes Tau: 1.00

(1)	(2)	(3)	(4)	(5)	(6)	(7)	(8)	(9)
15	4.9	1.6	0.6	0.2	0.1	-.-	-.-	-.-
30	9.5	3.1	1.1	0.4	0.1	-.-	-.-	-.-
45	13.7	4.5	1.5	0.5	0.2	0.1	-.-	-.-
60	17.7	5.8	1.9	0.7	0.2	0.1	-.-	-.-
90	24.9	8.0	2.7	0.9	0.3	0.1	-.-	-.-
120	31.2	9.8	3.3	1.1	0.4	0.1	-.-	-.-
150	36.8	11.4	3.8	1.3	0.4	0.1	-.-	-.-
180	41.6	12.8	4.2	1.4	0.5	0.2	0.1	-.-
210	45.9	14.0	4.6	1.5	0.5	0.2	0.1	-.-
240	49.7	15.0	4.9	1.6	0.6	0.2	0.1	-.-
300	56.1	16.7	5.4	1.8	0.6	0.2	0.1	-.-
360	61.1	18.0	5.9	2.0	0.7	0.2	0.1	-.-

(f)

Readout time: 5m 30s Tau: 1.00

(1)	(2)	(3)	(4)	(5)	(6)	(7)	(8)	(9)
15	4.4	1.3	0.4	0.1	-.-	-.-	-.-	-.-
30	8.5	2.5	0.8	0.2	0.1	-.-	-.-	-.-
45	12.4	3.7	1.1	0.3	0.1	-.-	-.-	-.-
60	16.0	4.7	1.4	0.4	0.1	-.-	-.-	-.-
90	22.5	6.5	1.9	0.6	0.2	0.1	-.-	-.-
120	28.2	8.0	2.4	0.7	0.2	0.1	-.-	-.-
150	33.2	9.4	2.8	0.8	0.3	0.1	-.-	-.-
180	37.6	10.5	3.1	0.9	0.3	0.1	-.-	-.-
210	41.6	11.5	3.4	1.0	0.3	0.1	-.-	-.-
240	45.0	12.4	3.7	1.1	0.3	0.1	-.-	-.-
300	50.9	13.8	4.1	1.2	0.4	0.1	-.-	-.-
360	55.5	14.9	4.4	1.3	0.4	0.1	-.-	-.-

Readout time: 6 minutes Tau: 1.00

(1)	(2)	(3)	(4)	(5)	(6)	(7)	(8)	(9)
15	4.0	1.1	0.3	0.1	-.-	-.-	-.-	-.-
30	7.7	2.1	0.6	0.2	-.-	-.-	-.-	-.-
45	11.1	3.0	0.8	0.2	0.1	-.-	-.-	-.-
60	14.4	3.8	1.0	0.3	0.1	-.-	-.-	-.-
90	20.2	5.3	1.4	0.4	0.1	-.-	-.-	-.-
120	25.4	6.6	1.8	0.5	0.1	-.-	-.-	-.-
150	30.0	7.7	2.1	0.6	0.2	-.-	-.-	-.-
180	34.0	8.6	2.3	0.6	0.2	-.-	-.-	-.-
210	37.6	9.4	2.5	0.7	0.2	0.1	-.-	-.-
240	40.7	10.2	2.7	0.7	0.2	0.1	-.-	-.-
300	46.1	11.4	3.0	0.8	0.2	0.1	-.-	-.-
360	50.3	12.3	3.3	0.9	0.2	0.1	-.-	-.-

* All entries in units of seconds.

$d \ln P/dt = 0.236$ min^{-1}, which assumes the Sun rises perpendicular to the horizon. For our data, however, the Sun's rising angle was 65° to the horizon, which introduces a simple correction factor of 0.9 to the rate. Correcting for the rising angle and converting to base 10 yields

$$(d \log P/dt)_0 = 0.092 \text{ min}^{-1}. \quad (11)$$

This simplified computation compares favorably with our empirically determined slope

$$d \log S/dt = 0.091 \text{ min}^{-1} \pm 0.006. \quad (12)$$

Note that Eq. (10) preserves a dependence on Z and φ in the form $(\varphi R_0/Z)$. This is why we chose a single intermediate Z for comparison with the data. Fortunately, Z and φ vary together and thus their ratio induces only a relatively weak dependence. For the standard atmosphere (NOAA 1976), Eq. (11) gives 0.064 min^{-1} for $Z=400$ km and 0.120 min^{-1} for $Z=100$ km. Of the four broadband filters in this study, the R band is the only one to display this trend of increasing slope toward sunrise (see Fig. 1), but the effect is not as pronounced as the standard atmosphere indicates.

Closer examination of the original simplifying assumptions reveal that they are also physically reasonable. We neglect the angular dependence of Rayleigh scattering because the angle between the shadow boundary and the line of sight to the zenith remains within 10% of 90°; the familiar $\sin^2\theta$ dependence for scattered radiation is correspondingly small. We neglect the 0.5° angular extent of the Sun because the Sun moves 20 times its diameter over the interval of the data. We take the shadow boundary to be sharp because at an altitude of 400 km, the width of Earth's penumbra is less than 2 km. Lastly, at 400 km,

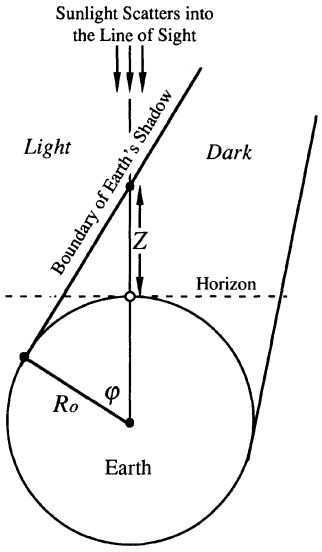

FIG. 2. Schematic of the geometry for the twilight sky (not to scale). For our derivation, we assume that the only contributing light source to the twilight sky is light that is scattered from outside of Earth's shadow into the column of atmosphere along the line of sight, (the zenith, for this figure). R_0 is Earth's radius, φ is the angle (as seen from the Earth's center) between the observation and the point on Earth that is experiencing sunrise, and Z is the distance from Earth's surface to the border of Earth's shadow as the shadow descends (or ascends) through the atmosphere. The observer's horizon is noted.

light refracted by the lower atmosphere penetrates only 15 km into the idealized shadow.

If the observer has reason to believe that the standard atmosphere applies in detail at a particular time or location, [complete with the small dependence on Z and φ in Eq. (10)], then the observer may still use Table 3, since it incorporates what we have determined to be the intermediate value of a slowly changing slope.

7. SUMMARY

We have provided a simple analytic expression [Eqs. (4) and (5)] plus a sample look-up table (Table 3) with which the observer can determine both the ideal exposure times and the total number of exposures that can be taken when seeking a series of twilight flatfields. We expect it to be most useful for large format CCDs, where the rapidly changing surface brightness of the dawn or dusk sky creates great uncertainty during the extended readout times. Observers who use CCDs with shorter readout times can also benefit from the efficiency provided by a predetermined exposure sequence. A simple FORTRAN 77 program to generate a formatted table of recommended exposures is available via anonymous FTP: astro.princeton.edu, file: /pub/twilight.f.

We thank Ed Turner for his comments on an earlier version of the manuscript and we thank Bruce Draine for his insights that enhanced Sec. 6 of this paper. Discussions with Ed Jenkins were also helpful. One of us (N.D.T.) gratefully acknowledges electronic mail conversations with Alistair Walker about the virtues and vices of the Tek 2 K chip. An anonymous referee made useful suggestions that helped to clarify our presentation in Sec. 3. This work was supported, in part, by NSF Grant No. AST-90-15827.

REFERENCES

Buil, C. 1992, CCD Astronomy: Construction and Use of an Astronomical CCD Camera, English translation (Willmann–Bell, Inc., Richmond), p. 253
Harding, P. 1992, private communication
Ingerson, T., Smith, D., Smith, R., Walker, A., & Weller, W. 1992, NOAO Newslett. No. 29, p. 15
Mackay, C. D. 1986, ARA&A, 24, 255
National Oceanic and Atmospheric Administration 1976, US Standard Atmosphere 1976 (US GPO, Washington, DC)(NOAA 1976), excerpted by Lide, D. R. 1992, for CRC Handbook of Chemistry and Physics, 72nd Edition (CRC Press, Boston), Sec. 14
U. S. Naval Observatory 1992, Astronomical Almanac (GPO, Washington, DC), Sec. A
Walker, A., Smith, R., Smith, D., & Ingerson, T. 1992, NOAO Newslett. No. 31, p. 10